Measurement of $\phi(1020)$ Meson Production in Neutral Current Deep Inelastic Scattering at HERA

B. B. Levchenko

Institute of Nuclear Physics, Moscow State University
119992 Moscow, Russia
For the ZEUS Collaboration

Abstract

First results on inclusive $\phi(1020)$ meson production in neutral current DIS have been obtained with the ZEUS detector at HERA using an integrated luminosity of 45 pb^{-1}. Cross sections have been measured in the range of the virtuality of the exchanged photon, $10 < Q^2 < 100$ GeV^2, and in restricted kinematic regions in transverse momentum, p_T, and pseudorapidity of the ϕ meson. The Monte Carlo models with the strange quark suppression factor as for e^+e^- annihilation overestimate the measured cross sections. A smaller value of the suppression factor reduces the predicted cross sections, but fails to reproduce the shapes of the measured ϕ meson differential cross sections.

1 Introduction

The valence quark content of proton is well established. However, the flavour composition of the sea quarks in proton is less understood. The main purpose of this paper is to investigate the sensitivity of the $\phi(1020)$ meson production in deep inelastic scattering (DIS) to the strange sea.

Strange particle production in inclusive DIS has already been studied at HERA using K^0 mesons and Λ baryons [2, 1]. In contrast to K^0 and Λ, ϕ meson is nearly a pure $s\bar{s}$ state due to the ideal mixing with the ω. In addition, the contribution to ϕ meson production from resonance decays is small.

Production of strange quarks in zeroth-order QCD for the quark-parton model (QPM) can be understood in terms of the hard scattering of a virtual photon on the proton strange sea, $\gamma^* s \to s$. The QCD Compton (QCDC) reaction, $\gamma^* s \to sg$, is a first-order QCD process, which is also determined by the strange sea. Another source of the strange quarks in first-order QCD is the Boson-Gluon Fusion (BGF) process ($\gamma^* g \to s\bar{s}$). In contrast to the QPM and QCDC processes, the BGF is determined by the gluon density in the proton. Hadronisation of the strange quarks produced in hard interactions can lead to the production of ϕ mesons. In addition, the hadronisation process itself also contributes to ϕ meson cross section even without the presence of strange quarks at the parton level. In Monte Carlo (MC) models based on the Lund fragmentation the ratio of strange particle to light non-strange particle production is parameterized by the strange suppression factor, $\lambda_s \equiv P_s/P_u$, where P_s (P_u) is the probability for creating s (u, d) quarks from the vacuum during the fragmentation.

Production of ϕ mesons in e^+e^- annihilation is well described by the MC models with $\lambda_s = 0.3$ [3]. The same hadronisation mechanism as in e^+e^- is used by the MC models to describe DIS events, thus it is expected that the contribution from the hadronisation process in the kinematic region of DIS events which is least affected by the proton remnants is well constrained from e^+e^- annihilations. In addition, selecting ϕ mesons with high p_T values minimizes the contribution from fragmentation. Therefore, the measurement of ϕ mesons in such kinematic regions can shed light on the strange quark production by hard interactions and the strange sea in the proton.

The strange quark densities are parameterized by the global QCD analyses of parton densities, CTEQ [4], MRST [5] and GRV [6]. In CTEQ and MRST, the strange quark density is defined at a low value of $Q^2 = Q_0^2$, where Q^2 is the virtuality of the exchanged boson. The s-quark density at higher Q^2 can be calculated by using the next-to-leading DGLAP evolution equation. The GRV [6] analysis has a different treatment of the strange sea: it assumes a vanishing strange quark density at a very low scale $Q^2 = \mu^2$. Then, the strange sea in GRV is generated using DGLAP purely dynamically and is a parameter-free prediction.

In this paper, ϕ mesons are measured in the central pseudorapidity region for relatively high transverse momenta, i.e. in the kinematic region which is least affected by the proton remnants. The differential cross sections are measured in Q^2 and Bjorken x, which are defined as $Q^2 = -q^2 = -(k - k^{'})^2$ and $x = Q^2/(2P \cdot q)$, where k and $k^{'}$ denote the four-momenta of the initial and final-state lepton, respectively, and P is the four-momentum of the proton. The ϕ mesons were identified through the decays $\phi \to K^+K^-$.

2 Data sample and analysis procedure

2.1 Experimental setup

During the 1995-1997 period, 45.0 ± 0.7 pb^{-1} of data were taken with a positron beam energy of 27.5 GeV and a proton beam energy of 820 GeV.

ZEUS is a multipurpose detector described in detail elsewhere [7]. Of particular importance for the present study are the central tracking detector and the calorimeter.

The central tracking detector (CTD) is a cylindrical drift chamber with nine superlayers covering the polar angle[1] region $15^o < \theta < 164^o$ and the radial range 18.2-79.4 cm. Each superlayer consists of eight sense wire layers. The transverse momentum resolution for charged tracks traversing all CTD layers is $\sigma(p_T)/p_T = 0.0058p_T \oplus 0.0065 \oplus 0.0014/p_T$ with p_T being the track transverse momentum (in GeV).

The CTD is surrounded by the uranium-scintillator calorimeter which is divided into three parts: forward, barrel and rear. The calorimeter is longitudinally segmented into electromagnetic and hadronic sections. The energy resolution of the calorimeter under test beam conditions is $\sigma_E/E = 0.18/\sqrt{E}$ for electrons and $\sigma_E/E = 0.35/\sqrt{E}$ for hadrons (with E in GeV).

[1]The ZEUS coordinate system is a right-handed Cartesian system, with the Z axis pointing in the proton beam direction, and the X axis pointing left towards the centre of HERA. The coordinate origin is at the nominal interaction point. The polar angle θ is defined with respect to the positive Z-direction. The pseudorapidity, η, is given by $-\ln(\tan \frac{\theta}{2})$.

2.2 Kinematic reconstruction and event selection

The kinematic variables Q^2 and x were reconstructed by the following methods:

- for the electron method (this method is specified with the subscript e), measurements of the energy and angle of the scattered positron were used;
- the double angle (DA) method [8] relies on the angles of the scattered positron and of the hadronic energy flow;
- the Jacquet-Blondel (JB) method [9] is based entirely on measurements of the hadronic system.

The DIS event selection contains the following requirements:

- $E_{e'} \geq 10$ GeV, $E_{e'}$ being the energy of the scattered positron in the calorimeter;
- $Q_e^2 \geq 10$ GeV^2; $2 \cdot 10^{-4} < x_e < 10^{-2}$; $y_e \leq 0.95$; $y_{\mathrm{JB}} \geq 0.04$;
- $40 \leq \delta \leq 60$ GeV, where $\delta = \sum E_i(1-\cos\theta_i)$, E_i is the energy of the ith calorimeter cell and the sum runs over all cells;
- a primary vertex position, determined from the tracks fitted to the vertex, in the range $\mid Z_{vertex} \mid < 50$ cm;
- the impact point (X, Y) of the scattered positron in the calorimeter must lie outside the ring centered on $X = Y = 0$ with radius 25 cm.

The reconstruction of the differential cross sections in the Q^2 and x variables was performed using the electron method, since it has the best resolution at relatively low Q^2 (< 100 GeV^2) values used in this paper.

3 Selection of the $\phi(1020)$ candidates

Charged tracks measured by the CTD and assigned to the primary event vertex were selected using the following requirements:

- the transverse momentum $p_T^{lab} > 200$ MeV, to ensure that the tracks are well measured;
- tracks that reach at least the third CTD superlayer were used,to restrict the study to a CTD region where track acceptance and resolution are high.

First, each pair of oppositely-charged tracks was combined to form a ϕ candidate. Both tracks were assigned the mass of a charged kaon and the invariant mass of the track pair was found. The combination was chosen with an invariant mass closest to the nominal $\phi(1020)$ mass.

The kinematic region permitted for ϕ candidates was: $1.7 < p_T(\phi) < 7$ GeV and $-1.7 < \eta(\phi) < 1.6$; $0.99 < M(\phi) < 1.06$ GeV. The asymmetric cut on $\eta(\phi)$ was used to avoid the very forward region of the CTD with large charged multiplicities in order to reduce the combinatorial background.

Figure 1 shows the invariant mass distribution for the ϕ candidates for $10 < Q^2 < 100$ GeV^2. The background from the wrong-charge combinations has significantly different shape and is not shown. The solid line is a fit using the relativistic Breit-Wigner (BW) function convoluted with a Gaussian distribution plus a term describing the background:

$$F(M) = (BW) \otimes (Gaussian) + a \cdot (M - 2m_K)^b, \tag{1}$$

where a and b are free parameters and m_K is the kaon mass. The peak and width of the Breit-Wigner function were fixed at the nominal PDG values [10] for the calculation of the differential cross sections. If the peak position is not fixed, the resulting fit gives 1019.2 ± 0.3 MeV, which agrees well with the present PDG value of 1019.417 ± 0.014 MeV [10]. The width of the Gaussian is 1.6 ± 0.3, consistent with the tracking resolution.

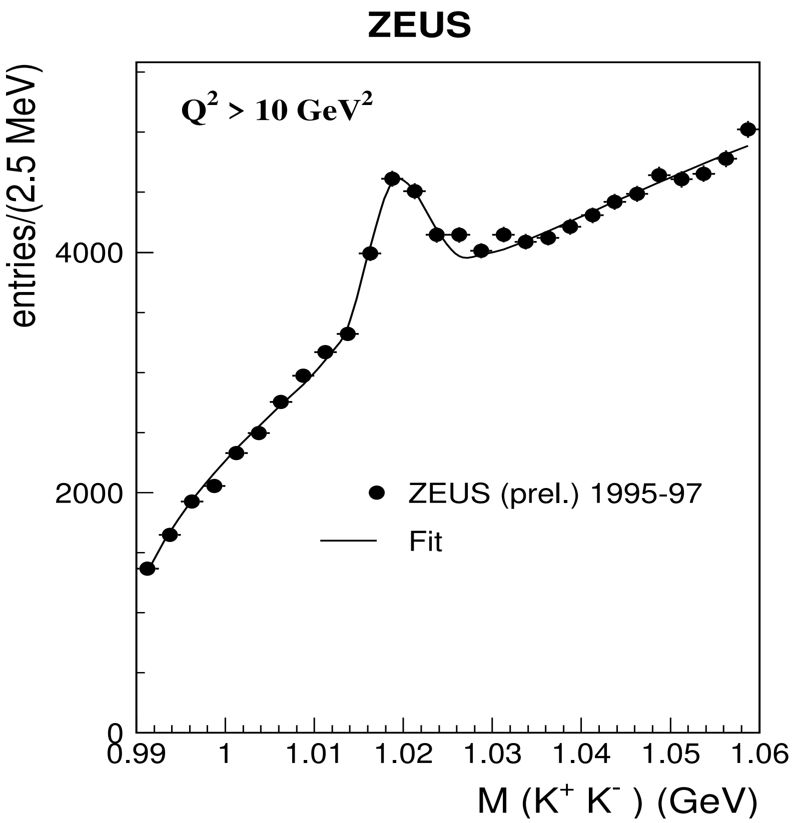

Figure 1: Data (points) for the invariant mass of the $\phi(1020)$ meson candidates. The solid line shows the result of the fit described in the text.

The total number of ϕ candidates determined from the fit described above is 5060 ± 216.

3.1 Event simulation

The data were compared to various leading-order MC models which generate entire hadronic final state systems in neutral current DIS events. These models are based on the parton-cascade approach to incorporate high-order QCD effects and realistic fragmentation. The MC events were generated with DJANGOH [11], LEPTO 6.5 [12] and ARIADNE [13].

The acceptance was calculated using the DJANGOH model interfaced with HERACLES 4.5.2 [14] in order to incorporate first-order electroweak corrections. The generated events were then passed through a full simulation of the detector using GEANT 3.13 [15] and processed with the same reconstruction program as that used for the real data. The detector-level MC samples were then selected in the same way as the data.

4 Systematic uncertainties

The systematic uncertainties on the measured cross sections were estimated from the following:

- event reconstruction and selection. Systematic checks were performed by varying the cuts on y_e, $y_{\rm JB}$, δ and the vertex position requirement ($y_e \leq 0.90$, $y_{JB} > 0.05$, $42 \leq \delta \leq 57$ GeV, $| Z_{vertex} |< 45$ cm). The radius cut for the position of the scattered positron in the calorimeter was raised by 1 cm. The minimum value of the energy of the scattered lepton was increased by 1 GeV. The positron energy scale was changed within the $\pm 2\%$ uncertainty;
- the DA-method was used to reconstruct the kinematic variables;
- The minimum transverse momentum for a K-meson candidate was raised and lowered by 100 MeV. Tracks were required to have $| \eta |< 1.75$, in addition to the requirement of 3 CTD superlayers.
- The shape of the background was varied. To exclude a possible contribution from exclusive ϕ meson production, which is not well described by MC models for inclusive DIS, events were selected with the number of charged tracks larger than two.

The overall systematic uncertainty was determined by adding the above uncertainties in quadrature. The normalization uncertainties due to the luminosity measurement error, and those due to the ϕ decay branching ratios [10] were not included in the systematic uncertainties.

5 Results

The cross sections for a given observable Y were determined from

$$\frac{d\sigma}{dY} = \frac{N}{A \cdot \mathcal{L} \cdot B \cdot \Delta Y} \ ,$$

where N is the number of ϕ events determined from the fits in a bin of size ΔY, A is the acceptance (which takes into account migrations, efficiencies and radiative effects for that bin) and $\mathcal{L}$ is the integrated luminosity. The branching ratio, B, for the decay channel $\phi \to K^+K^-$ is taken to be 0.492 ± 0.007, in accordance with the PDG [10].

The overall acceptance for $10 < Q^2 < 100$ GeV^2, $2 \cdot 10^{-4} < x < 10^{-2}$, $0.04 < y < 0.95$, $1.7 < p_T(\phi) < 7$ GeV and $-1.7 < \eta(\phi) < 1.6$ estimated with DJANGOH was 51%. The total cross section measured in this region is

$$\sigma(e^+p \to e^+\phi X) = 0.513 \pm 0.022(\text{stat.})^{+0.006}_{-0.010}(\text{syst.})\ \text{nb.} \tag{2}$$

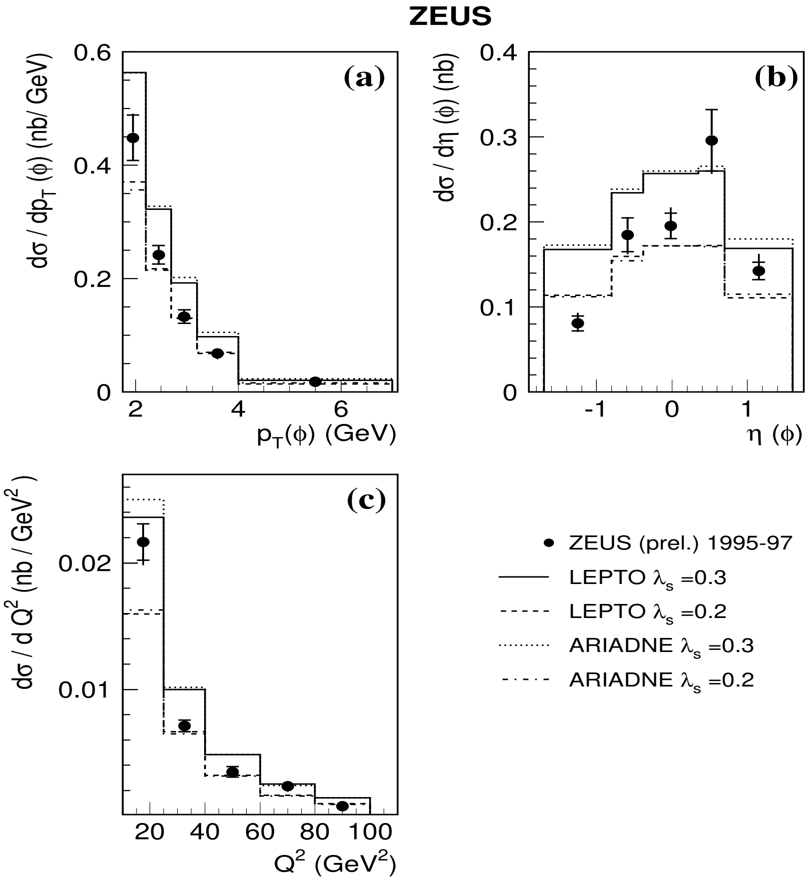

Figure 2: Differential ϕ meson cross sections as functions of p_T, η and Q^2, compared to leading-order MC models with the CTEQ5D parton density and two values of the strange suppression factor. The full error bars include the systematic uncertainties, which are typically negligible compared to the statistical errors.

Figure 2 shows the differential cross sections as a function of $p_T(\phi)$, $\eta(\phi)$ and Q^2, compared to LEPTO and ARIADNE with the CTEQ5D parton distribution function and two different values of λ_s. For the default value, $\lambda_s = 0.3$, the MC models have larger overall ϕ-meson cross sections than the data, although the shapes of the cross sections are reasonably reproduced.

In previous studies of neutral kaons and Λ baryons at HERA [1, 2, 16] it was found that decreasing λ_s from its standard value to $\lambda_s = 0.2$ improved the agreement between MC models and the data. Figure 2 shows that a reduction of the strangeness suppression from 0.3 to a value of 0.2 decreases the MC cross sections. Note that this reduction of the value of λ_s changes the shapes of the MC cross sections[2], rather than the overall normalization only. The MC models with the lower suppression factor have a harder $p_T(\phi)$ spectrum and fail to describe the data at lowest Q^2. Good agreement between the

[2]In contrast, the shapes of the distributions for K^0 do not depend on the chosen λ_s [1], since K^0 mesons are mainly produced during the hadronisation process.

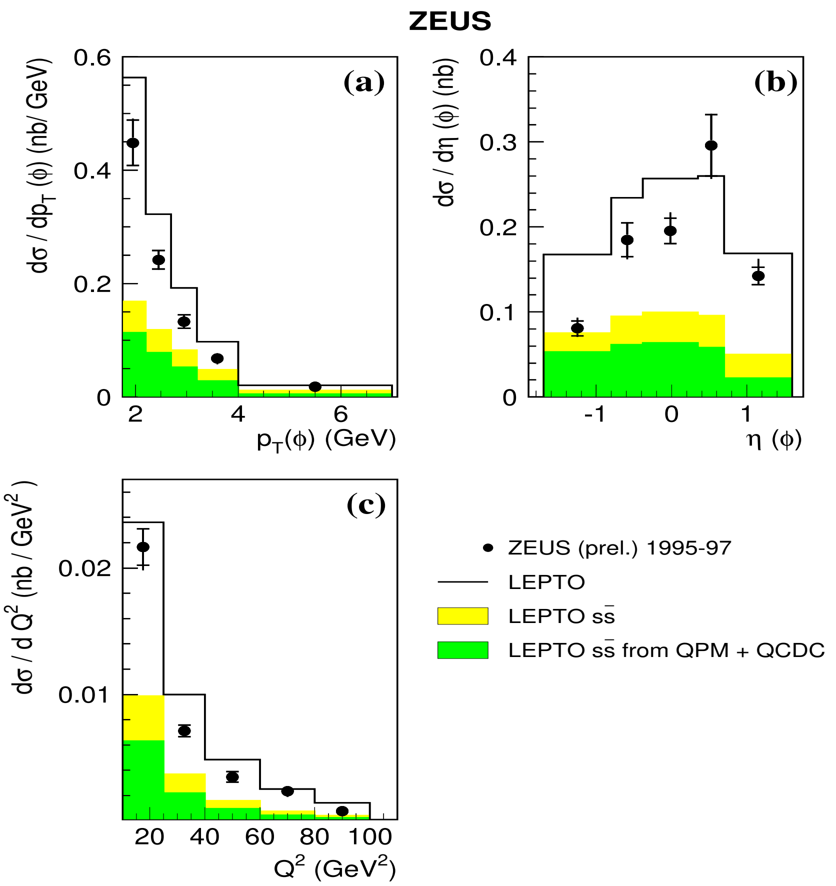

Figure 3: Same as Fig. 2, but the data are compared to the contribution from events with an $s\bar{s}$ pair produced in hard interactions via QPM, QCDC and BGF processes (LEPTO $s\bar{s}$). The CTEQ5D parton density and $\lambda_s = 0.3$ were used. The QPM and QCDC expectation for a strange sea contribution is also shown (LEPTO $s\bar{s}$ from QPM + QCDC).

MC and data for the lowest $p_T(\phi)$ and Q^2 regions can be obtained using $\lambda_s = 0.25$. In this case, however, the MC models overestimate the cross sections for the high $p_T(\phi)$ and Q^2 regions. The use of the leading-order structure function, CTEQ5L, gives similar results to those shown in Fig. 2.

Figure 3 shows the same data as in Fig. 2, but LEPTO with CTEQ5D and $\lambda_s = 0.3$ is used to illustrate the contributions of hard interactions in which an $s\bar{s}$ pair is produced in QPM, QCDC and BGF processes. The contribution of the strange sea determined by QPM and QCDC processes, in which the flavour of the struck quark is strange (anti-strange), is shown separately. This contribution rises with increasing $p_T(\phi)$. The difference between the two shaded histograms shown in Fig. 3 indicates the BGF contribution to the strange quark production. For ARIADNE, the contribution to the ϕ meson cross sections from the BGF process is slightly higher (not shown).

The main purpose of this paper is to investigate the sensitivity of ϕ production to the

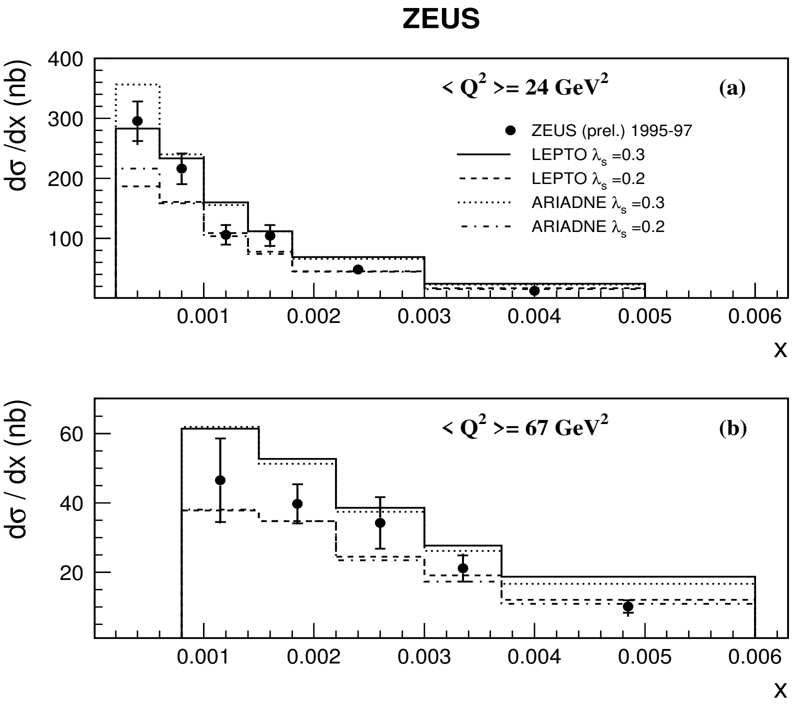

Figure 4: The differential ϕ meson cross section as a function of x for data and MC predictions; (**a**) for $10 < Q^2 < 35$ GeV ^{2}; and (**b**) for $35 < Q^2 < 100$ GeV ^{2}. The inner error bars on the data show the statistical uncertainties and the full error bars include the systematic uncertainties.

strange sea in the proton. The most natural variable for this is Bjorken x, because the hadronisation process and resonance decays are expected to have little dependence on x. In contrast, the s-quark density increases with a decrease of x. The BGF contribution, however, also increases with decreasing x due to the rise of the gluon density; thus the dependence of the ϕ meson cross section as a function of x should be sensitive to both the strange sea and the gluon density. While the interpretation in terms of the leading-order MC models involves both densities, the physics of strangeness production is the same: interactions of the virtual photon with a strange quark pair from a gluon.

The differential cross sections as a function of x for $10 < Q^2 < 35$ GeV^2 and $35 < Q^2 < 100$ GeV^2 are shown in Figs. 4(a) and (b), respectively. The ϕ meson differential cross section increases when x decreases. The MC models with $\lambda_s = 0.3$ overestimate the cross sections. Using a smaller value of 0.2 reduces the predicted cross sections. However, the MC models with such a suppression factor underestimate the cross sections for $x < 0.001$.

Figure 5 again illustrates the contributions from the hard scatterings in which an $s\bar{s}$ pair is produced at the parton level. The LEPTO model with the CTEQ5D parton densities and $\lambda_s = 0.3$ was used. The contribution from the QPM, QCDC, and BGF processes rises with decreasing x, which is due to a similar rise of the s-quark and gluon density in the proton.

Similar comparisons have been performed using the LEPTO and ARIADNE models based on the GRV98 [6] parton density function. The MC predictions with $\lambda_s = 0.3$ were found to be in good agreement with the measured cross sections, both for the shapes and the normalizations. This is due to the fact that the MC models with GRV98 predict a lower total inclusive DIS cross section (i.e. F_2) than for CTEQ5D.

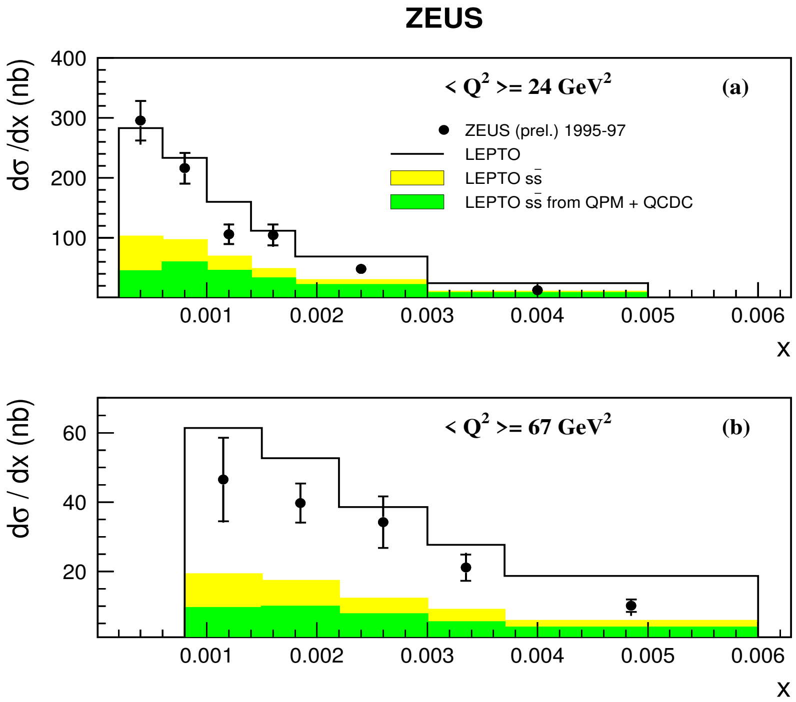

Figure 5: Same as Fig. 4, but the data are compared to the contribution from events with an $s\bar{s}$ pair produced in hard interactions via QPM, QCDC and BGF processes (LEPTO $s\bar{s}$). The CTEQ5D parton density and $\lambda_s = 0.3$ were used. The QPM and QCDC expectation for a strange sea contribution is also shown (LEPTO $s\bar{s}$ from QPM + QCDC).

6 Conclusion

Inclusive ϕ meson cross sections in restricted kinematic regions have been measured in deep inelastic scattering for $10 < Q^2 < 100$ GeV^2 with the ZEUS detector at HERA. The MC predictions with CTEQ5D and $\lambda_s = 0.3$ overestimate the measured cross sections. A smaller value of $\lambda_s = 0.2$ reduces the MC cross sections. In this case, however, the MC models predict different shapes of the cross sections, underestimating the data for low values of $p_T(\phi)$, Q^2 and x, which are most strongly affected by the contribution from the hadronisation process. Therefore, the results indicate the need for an adjustment of not only the fragmentation suppression factor λ_s, but also of the strange quark density in the proton.

Acknowledgements. This study was performed together with S. Chekanov and I would like to express him and the QCD working group my gratitude for many stimulating discussions. The strong support and encouragement of the DESY Directorate have been invaluable.

References

[1] ZEUS Collaboration, M. Derrick et al., Phys. Lett. B 354 (1995) 163

[2] H1 Collaboration, S. Aid et al., Nucl. Phys. B 480 (1996) 3

[3] OPAL Collaboration, P.D. Acton et al., Z. Phys. C 56 (1992) 521;
OPAL Collaboration, R. Akers et al., Z. Phys. C 68 (1995) 1;
ALEPH Collaboration, D. Buskulic et al., Z. Phys. C 69 (1996) 379;
DELPHI Collaboration, P. Abreu et al., Z. Phys. C 73 (1996) 61;
OPAL Collaboration, K. Ackerstaff et al., Eur. Phys. J. C 4 (1998) 19;
SLD Collaboration, K. Abe et al., Phys. Rev. D 59 (1999) 052001

[4] H.L. Lai et al., Eur. Phys. J. C 12 (2000) 375

[5] A.D. Martin at al., Eur. Phys. J. C 4 (1998) 463

[6] M. Glück, E. Reya and A. Vogt, Eur. Phys. J. C 5 (1998) 461

[7] ZEUS Collaboration, M. Derrick et al., Phys. Lett. B 293 (1992) 465;
ZEUS Collaboration, M. Derrick et al., Z. Phys. C 63 (1994) 391

[8] S. Bentvelsen, J. Engelen and P. Kooijman, *Proceedings of the 1991 Workshop on Physics at HERA*, DESY, W. Buchmüller and G. Ingelman (eds.), (1992) p. 23; K. C. Hoeger, *ibid.*, p.43

[9] F. Jacquet and A. Blondel, in: *Proceedings of the study for an ep facility for Europe*, U. Amaldi (ed.), DESY 79-48 (1979) p. 391

[10] Particle Data Group, C. Caso et al., Eur. Phys. J. C 3 (1998) 1

[11] H. Spiesberger et al., `http : //www.desy.de/~hspiesb/djangoh.html`

[12] LEPTO 6.5, G. Ingelman, A. Edin and J. Rathsman, Comp. Phys. Comm. 101 (1997) 108

[13] ARIADNE 4.07, L. Lönnblad, Comp. Phys. Comm. 71 (1992) 15

[14] HERACLES 4.5.2, A. Kwiatkowski, H.-J. Möhring and H. Spiesberger, Comp. Phys. Comm. 69 (1992) 155

[15] R. Brun et al., GEANT3, CERN DD/EE/84-1

[16] ZEUS Collaboration, J. Breitweg et al., Eur. Phys. J. C 2 (1998) 77